High-order above-threshold ionization in elliptically polarized laser fields: Identifying the recollision time

Zhangjin Chen, Qiongmin Ding, Qinghua Chen, and Shuqi Li

Department of Physics, College of Science, Shantou University, Shantou, Guangdong 515063, People's Republic of China

Fang Liu

Helmholtz-Institut Jena, 07743 Jena, Germany;
Theoretisch-Physikalisches Institut, Friedrich-Schiller-Universität Jena, 07743 Jena, Germany;
and GSI Helmholtzzentrum für Schwerionenforschung GmbH, 64291 Darmstadt, Germany

Huipeng Kang

State Key Laboratory of Magnetic Resonance and Atomic and Molecular Physics, Wuhan Institute of Physics and Mathematics, Innovation Academy for Precision Measurement Science and Technology, Chinese Academy of Sciences, Wuhan 430071, China

Toru Morishita

Institute for Advanced Science, The University of Electro-Communications, 1-5-1 Chofu-ga-oka, Chofu-shi, Tokyo 182-8585, Japan

Jing Chen

Department of Modern Physics, and Hefei National Research Center for Physical Sciences at the Microscale and School of Physical Sciences, University of Science and Technology of China, Hefei 230026, People's Republic of China
and Hefei National Laboratory, University of Science and Technology of China, Hefei 230088, China

We simulate the two-dimensional high-energy photoelectron momentum distributions (PMDs) for high-order above threshold ionization (HATI) of hydrogen atoms in intense elliptically polarized laser fields by using the strong-field approximation and solving the time-dependent Schrödinger equation. It is found that the centers of the left- and right-side circular rescattered ridges in the PMDs due to elastic collision of the returning electron with the parent ion, that locate on the polarization axis for linearly polarized laser field, move slightly below and above the major polarization axis, respectively, for elliptically polarized laser fields. We suggest that, by analyzing the center shift of the measured PMDs for HATI in elliptically polarized fields, one can identify the recollision time.

I. INTRODUCTION

Above-threshold ionization (ATI) is a fundamental process resulting from the interaction of an intense laser field with matter. During ATI more photons are absorbed from the laser field than is necessary for ionization and the emitted electron spectrum consists of peaks separated by the photon energy [1]. The ionized electron wave packets can also trigger a range of dynamics in strong-field and attosecond physics [2,3]. The force on the electron from the field may pull it back to scatter on the parent ion. If the returning electron recombines with the ion, high-order harmonic generation (HHG) occurs in which its entire energy is emitted as one high-energy photon [4]. The returning electron can also elastically rescatter off the parent ion, move away from it, and reach the detector with a higher energy: This is the high-order ATI (HATI) process [5]. Another particularly important laser-induced process is nonsequential double ionization (NSDI) including recollision direct ionization (RDI) and recollision excitation with subsequent ionization (RESI) [6,7].

In the past decades, both ATI and HATI in linearly polarized laser fields have been extensively studied. In contrast to the case of linear polarization, the use of elliptically polarized laser fields has added more dimensions to study strong laser-field ionization and has attracted particular attention [8–20], which gave rise to more features and properties that were not accessible with a linearly polarized laser field. One decade ago, the experimental measurements of the photoelectron or ion angular distributions of noble gases in intense elliptically polarized laser fields were performed. It was found that, for ellipticity <0.3, the measured photoelectron or ion angular distributions in the low-energy regime (below $2U_p$, where U_p is the ponderomotive energy) exhibit Coulomb asymmetry [9,10]. This prominent feature was first attributed to the initial longitudinal momentum spread of the electron at the tunnel exit in the ionization of He [9]. Interestingly, it was later argued that the effect of the initial longitudinal momentum spread was not observed in the ionization of Ne [10]. Instead, it was shown that the tunneling time and initial transverse momentum have dominant roles on Coulomb asymmetry [10]. In the mean time, an ellipticity-resolved study of HATI was presented by Lai *et al.* who measured the photoelectron energy spectra of Ar, Kr, and Xe along the major polarization

axis [12] in which it was demonstrated that elliptical polarization favors long quantum orbits in HATI. Later on, two-dimensional (2D) photoelectron momentum distributions (PMDs) for HATI from single ionization of atoms in intense elliptically polarized laser fields were investigated by Yu *et al.* [13] using a three-dimensional semiclassical model. It was found that the relative contribution of the second recollision to the yield of the high-energy photoelectrons increased with the ellipticity. Recently, through studying the angle-resolved momentum distributions of the rescattered electrons from HATI of negative ions by an elliptically polarized laser field, Milošević and Becker discussed the contribution of negative-travel-time quantum orbits in complex space and time [16].

While all laser-induced rescattering processes can be qualitatively interpreted by the three-step quasiclassical recollision model [21,22], recollision time and electron trajectories play a crucial role in better understanding the underlying mechanisms. In the case of linear polarization, it has been recognized that the recombination of long-trajectory electrons with the parent ion usually does not contribute to the macroscopic HHG spectra based on the analysis of phase matching [23]. In contrast, the contribution to HATI from the short-trajectory electrons can be ignored since the long-trajectory electrons have much higher ionization rate [24]. This indicates that elastic recollisions responsible for HATI take place more likely after the field zero crossing. However, the information of recollision time is hidden to NSDI with linearly polarized light. Recently, Kang *et al.* [17,18] reported a joint experimental and theoretical investigation of NSDI by elliptically polarized laser pulses. They studied double ionization as a function of the ellipticity of the driving field and showed that recollisions are more likely to occur after the zero crossing of the electric field along major polarization for higher ellipticities.

In the present paper we simulate the PMDs of HATI for ionization of H atoms in elliptically polarized laser fields by using the strong-field approximation (SFA) and solving the time-dependent Schrödinger equation (TDSE). By analyzing the position of the rescattering center in the momentum space, it can be deduced that recollisions for HATI in elliptically polarized laser fields are more likely to occur *before* the zero crossing of the electric field along major polarization, which is different from the situation for NSDI as indicated in [17,18].

The remainder of the present paper is arranged as follows. The theoretical methods are presented in Sec. II. The simulated results are shown and discussed in Sec. III. Finally, our conclusions are given in Sec. IV.

Atomic units (a.u.) ($\hbar = |e| = m = 4\pi\epsilon_0 = 1$) are used throughout the paper unless otherwise indicated.

II. THEORETICAL METHODS

In this paper, we consider HATI of H in elliptically polarized laser pulses. The electric field of the elliptically polarized light in the (z, y) plane is given by

$$\boldsymbol{F}(t) = F_0 \frac{a(t)}{\sqrt{1 + \varepsilon^2}} [\cos(\omega t + \varphi)\hat{z} - \varepsilon \sin(\omega t + \varphi)\hat{y}], \quad (1)$$

where ε is the ellipticity, ω is the carrier frequency, and φ is the carrier-envelope phase which is set to zero here. The envelope

function $a(t)$ is chosen as

$$a(t) = \cos^2\left(\frac{\pi t}{T}\right) \quad (2)$$

for the time interval $(-T/2, T/2)$ and zero elsewhere. Here, T is defined as the (full) duration of the laser pulse. With this definition of the laser field, the z and y axes are the beam's major and minor axes, respectively. The vector potential of the laser field $\boldsymbol{F}(t)$ is given by

$$\boldsymbol{A}(t) = -\int_{-\infty}^{t} dt' \boldsymbol{F}(t'). \quad (3)$$

Two methods are used in the numerical simulations of the PMDs for HATI of H. One is based on the SFA and the other is to numerically integrate the TDSE.

A. Strong-field approximation

The total Hamiltonian of an atom interacting with the laser field is given by

$$H(t) = H_a + H_i(t), \quad (4)$$

where

$$H_a = -\frac{1}{2}\nabla^2 + V(\boldsymbol{r}) \quad (5)$$

is the atomic Hamiltonian, and

$$H_i(t) = \boldsymbol{r} \cdot \boldsymbol{F}(t) \quad (6)$$

is the laser-electron interaction in the length gauge and the dipole approximation. The exact transition amplitude of an ATI electron from the initial bound state $\Psi_0(t')$ to final state $\Psi_p(t)$ having the asymptotic momentum $\boldsymbol{p}$ can be expressed as

$$f(\boldsymbol{p}) = -i \lim_{t \to \infty} \int_{-t}^{t} dt' \langle \Psi_p(t)|U(t, t')H_i(t')|\Psi_0(t')\rangle. \quad (7)$$

Here $U(t, t')$ is the time-evolution operator of the total Hamiltonian and satisfies the Dyson equation

$$U(t, t') = U_F(t, t') - i \int_{t'}^{t} dt'' U_F(t, t'')VU(t'', t'), \quad (8)$$

where $U_F(t, t')$ is the time-evolution operator that corresponds to the Hamiltonian of a free electron in the laser field, which is

$$H_F = -\frac{1}{2}\nabla^2 + H_i. \quad (9)$$

The eigenstates of the TDSE with the Hamiltonian $H_F(t)$ are the Volkov states

$$|\chi_p(t)\rangle = |\boldsymbol{p} + \boldsymbol{A}(t)\rangle \exp[-iS_p(t)], \quad (10)$$

where $|\boldsymbol{k}\rangle$ is a plane-wave ket vector such that

$$\langle \boldsymbol{r}|\boldsymbol{k}\rangle = \frac{1}{(2\pi)^{3/2}} \exp(i\boldsymbol{k} \cdot \boldsymbol{r}), \quad (11)$$

and the action is given by

$$S_p(t) = \frac{1}{2} \int_{-\infty}^{t} dt' [\boldsymbol{p} + \boldsymbol{A}(t')]^2. \quad (12)$$

The Volkov time-evolution operator is

$$U_F(t, t') = \int d\boldsymbol{k} |\chi_{\boldsymbol{k}}(t)\rangle \langle \chi_{\boldsymbol{k}}(t')|. \tag{13}$$

In SFA, $\langle \Psi_{\boldsymbol{p}}(t)|U(t, t')$ is replaced by $\langle \chi_{\boldsymbol{p}}(t)|U(t, t')$ in Eq. (7). With the full time-evolution operator $U(t, t')$ truncated after the second term, the SFA probability amplitude may be decomposed into the contributions of direct and rescattered electrons which are referred to as SFA1 and SFA2, respectively,

$$f_{\text{SFA}}(\boldsymbol{p}) = f_{\text{SFA1}}(\boldsymbol{p}) + f_{\text{SFA2}}(\boldsymbol{p}), \tag{14}$$

where the first term

$$f_{\text{SFA1}}(\boldsymbol{p}) = -i \int_{-\infty}^{\infty} dt \langle \chi_{\boldsymbol{p}}(t)|H_i(t)|\Psi_0(t)\rangle \tag{15}$$

corresponds to the standard SFA for the direct ATI, and the second term

$$f_{\text{SFA2}}(\boldsymbol{p}) = -\int_{-\infty}^{\infty} dt \int_{t}^{\infty} dt' \int d\boldsymbol{k} \langle \chi_{\boldsymbol{p}}(t')|V|\chi_{\boldsymbol{k}}(t')\rangle$$
$$\times \langle \chi_{\boldsymbol{k}}(t)|H_i(t)|\Psi_0(t)\rangle \tag{16}$$

is the first-order correction to the standard SFA accounting for HATI. Obviously, SFA2 consists of ionization, propagation in the continuum, and elastic scattering of the returning electron with the parent ion.

For hydrogen-like atoms, the ground-state wave function takes the form

$$\Psi_0(\boldsymbol{r}, t) = 2Z^{3/2} \exp(-Zr) Y_{00}(\hat{\boldsymbol{r}}) \exp(iI_p t), \tag{17}$$

where Z is the charge of nucleus and I_p is the binding energy of the electron. The rescattering potential $V(\boldsymbol{r})$ is a pure Coulomb potential

$$V(\boldsymbol{r}) = -\frac{Z}{r}. \tag{18}$$

After performing integrations over space coordinates in Eqs. (15) and (16) analytically, we obtain

$$f_{\text{SFA1}}(\boldsymbol{p}) = -\frac{8\sqrt{2}}{\pi} Z^{5/2} \int_{-\infty}^{\infty} dt \exp[iS_{\boldsymbol{p}}(t)] \exp(iI_p t)$$
$$\times \frac{\boldsymbol{F}(t) \cdot [\boldsymbol{p} + \boldsymbol{A}(t)]}{\{Z^2 + [\boldsymbol{p} + \boldsymbol{A}(t)]^2\}^3}, \tag{19}$$

and

$$f_{\text{SFA2}}(\boldsymbol{p}) = -i\frac{4\sqrt{2}}{\pi^3} Z^{7/2} \int_{-\infty}^{\infty} dt \int_{-\infty}^{t} dt' \int d\boldsymbol{k}$$
$$\times \exp\{-i[S_{\boldsymbol{k}}(t) - S_{\boldsymbol{p}}(t)]\} \exp[iS_{\boldsymbol{k}}(t')] \exp(iI_p t')$$
$$\times \frac{1}{\alpha^2 + (\boldsymbol{k} - \boldsymbol{p})^2} \frac{\boldsymbol{F}(t') \cdot [\boldsymbol{k} + \boldsymbol{A}(t')]}{\{Z^2 + [\boldsymbol{k} + \boldsymbol{A}(t')]^2\}^3}. \tag{20}$$

In Eq. (20) α is a parameter introduced to avoid the singularity in the integrand. Actually, to obtain Eq. (20), the pure Coulomb potential in Eq. (18) is replaced by the Yukawa potential with a damping parameter α,

$$\tilde{V}(\boldsymbol{r}) = -\frac{Z}{r} e^{-\alpha r}. \tag{21}$$

It should be noted that the results depend on the value of α, but the dependence is relatively weak, affecting mainly the magnitude but not the structure of momentum distributions. Here, we choose $\alpha = 1$. The integral over the intermediate electron momenta $\boldsymbol{k}$ in Eq. (20) is approximated using the saddle-point method, so that only the twofold time integral is calculated numerically. The method used to evaluate SFA2 can be found in [25,26].

B. Time-dependent Schrödinger equation

Within the dipole approximation and the length gauge, the TDSE for an electron under the influence of a classical electromagnetic field reads

$$i\frac{\partial}{\partial t}\Psi(\boldsymbol{r}, t) = [H_a + H_i]\Psi(\boldsymbol{r}, t). \tag{22}$$

We solve the TDSE by using the second-order split-operator method combined with the R-matrix propagation method [27] generalized for the elliptically polarized laser pulses. The method was used for circularly polarized laser pulses in [28].

The probability amplitude for detecting an electron with momentum $\boldsymbol{p}$ at the end of the pulse is given by

$$f_{\text{TDSE}}(\boldsymbol{p}) = \langle \Phi_{\boldsymbol{p}}^- | \Psi(t = T/2) \rangle, \tag{23}$$

where $\Phi_{\boldsymbol{p}}^-$ is the scattering *out* eigenstate of the field free Hamiltonian, satisfying the equation

$$H_a \Phi_{\boldsymbol{p}}^- = E \Phi_{\boldsymbol{p}}^-, \tag{24}$$

where $E = p^2/2$ is the photoelectron energy.

III. RESULTS AND DISCUSSION

We simulate the PMDs for HATI of H in both linearly and elliptically polarized laser fields. In all the calculations, the intensity and the wavelength of the laser fields are 1×10^{14} W/cm^2 and 800 nm, respectively.

Our goal is to identify the favorite recollision time in HATI by elliptically polarized laser fields. We focus on the back rescattering ridges and consider large scattering angles with small ellipticities. To this end, we start with the case of linear polarization. In Fig. 1(a) we show the electric field and the corresponding vector potential for a three-cycle linearly polarized laser pulse, and the PMD in the plane containing the polarization axis for HATI of H by the electric field plotted in Fig. 1(a) is displayed in Fig. 1(b). The results shown in Fig. 1(b) are obtained from SFA2 which only accounts for rescattering of the ionized electron off the parent ion. Since the electron yield drops very rapidly with energy [26], for the sake of better visibility, in Fig. 1(b) only the parts of the PMD with photoelectron energy larger than $2U_p$ are shown. As expected, for linear polarization the PMD exhibits the characteristic form of a figure eight, elongated in the polarization direction, which has been well understood for more than a decade [24,26]. As demonstrated in Fig. 1(a), based on classical theory electrons that are released near the peak of the electric field around t_1 (t_2) will return to the origin along $-z$ ($+z$) at a time around the field crossing t_3 (t_4) when the vector potential is negative (positive). The elastic scattering of the returning electron with the parent ion that takes place at the
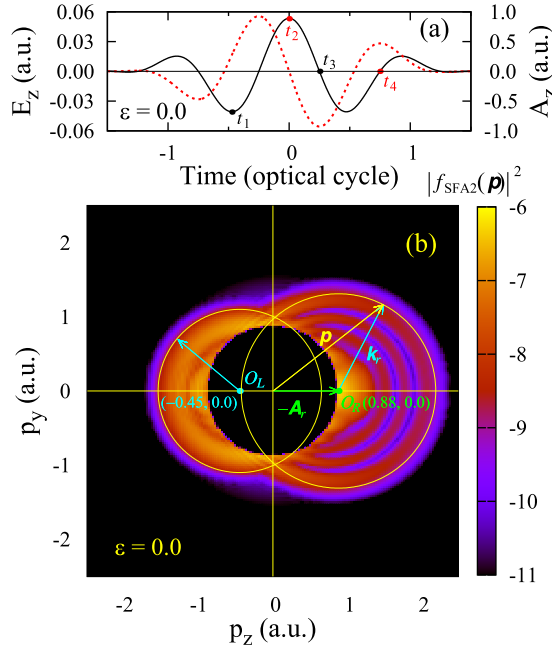
FIG. 1. (a) Electric field (solid curve and left vertical axis) and vector potential (dotted curve and right vertical axis) for a linearly polarized laser pulse with a full duration of three optical cycles at an intensity of 1×10^{14} W/cm^2 and a wavelength of 800 nm. (b) Two-dimensional photoelectron momentum distribution parallel and perpendicular to the polarization direction with photoelectron energy larger than $2U_p$ for single ionization of atomic hydrogen in the laser pulse depicted in panel (a). The results are obtained from SFA2. The right- and left-side circles represent the elastic scattering of a returning electron with the parent ion at recollision times around t_3 and t_4, respectively.

recollision time t_3 (t_4) forms the right-side (left-side) circular ring in the PMD, as shown in Fig. 1(b). In addition, the scattering circles are offset from the origin by the vector $-\boldsymbol{A}_r$, where $\boldsymbol{A}_r \equiv \boldsymbol{A}(t_r)$ with t_r the returning time at which recollision takes place. As indicated in Fig. 1(b), the centers of the right- and left-side circles are shifted, along the polarization direction, from the origin by 0.88 and -0.45, which are close to the local maximum values of the vector potential around t_3 and t_4, respectively. Owing to momentum conservation [29] the momentum $\boldsymbol{p}$ of the photoelectron is given by $\boldsymbol{p} = -\boldsymbol{A}_r + \boldsymbol{k}_r$, where $\boldsymbol{k}_r$ is the momentum of the rescattering electron.

Next we consider HATI of H by an elliptical polarized laser pulse. Here the ellipticity is 0.3, and the other laser parameters are the same as in Fig. 1. The electric field and the corresponding vector potential together with the PMD in the polarization plane are displayed in Fig. 2. One can see that the PMD in Fig. 2(c) under elliptical polarization exhibits a similar pattern to that in Fig. 1(b) with linear polarization although the total amount of high-energy photoelectrons drops about one order of magnitude. This trend was also found in the simulations based on a semiclassical model [13]. Whereas, while the right- and left-side circles are still attributed to the elastic collisions (taking place around the times of t_3 and t_4, respectively) of the returning electron with the parent ion, the PMD in Fig. 2(c) is obviously different from that in Fig. 1(b). The center of the right-side (left-side) circle moves slightly off
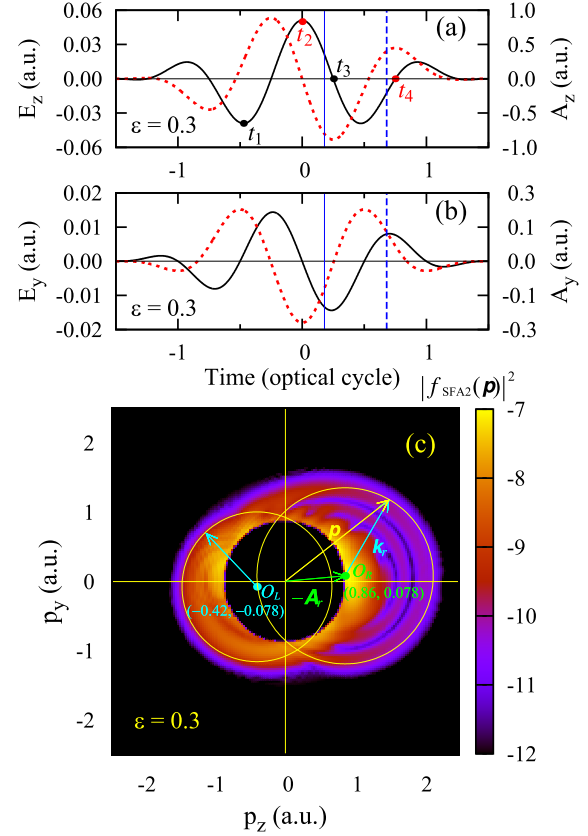

FIG. 2. Electric field (solid curve and left vertical axis) and vector potential (dotted curve and right vertical axis) along (a) the major axis (the z axis) and (b) the minor axis (the y axis) for an elliptically polarized laser pulse with a full duration of three optical cycles. The ellipticity is 0.3 here. The intensity and wavelength of the laser field are as in Fig. 1. The vertical lines show the recollision times before the E_z field zero crossing. (c) Two-dimensional photoelectron momentum distribution in the polarization plane with photoelectron energy larger than $2U_p$ for single ionization of atomic hydrogen in the laser pulse depicted in panels (a) and (b). The results are obtained from SFA2. The right- and left-side circles with the centers slightly above and below the major polarization axis represent the elastic scattering of a returning electron with the parent ion at recollision times before t_3 and t_4, respectively.

the p_z axis to the first (third) quadrant with a small positive (negative) momentum along the minor polarization axis.

Again, according to the classical rescattering model, the center of the circle is located at $[-A_z(t_r), -A_y(t_r)]$. Take the right-side circle in Fig. 2(c) as an example, the center of the circle is at (0.86, 0.078). As previously mentioned, the electron initially born near the peak of the E_z field around t_1 returns to the origin along $-z$ at a time around E_z zero crossing t_3. Because the recollision time is around the E_z field zero crossing, the value of $A_z(t_r)$ at the recollision time t_r is close to the peak vector potential, and it keeps negative no matter the recollision occurs before or after the E_z field zero crossing, as shown in Fig. 2(a). However, as one can see in Fig. 2(b), the recollision occurring before or after the E_z zero crossing corresponds to negative or positive $A_y(t_r)$. From Fig. 2(c), it can be deduced that $A_y(t_r) < 0$, which clearly indicates that the recollision takes place before the E_z field
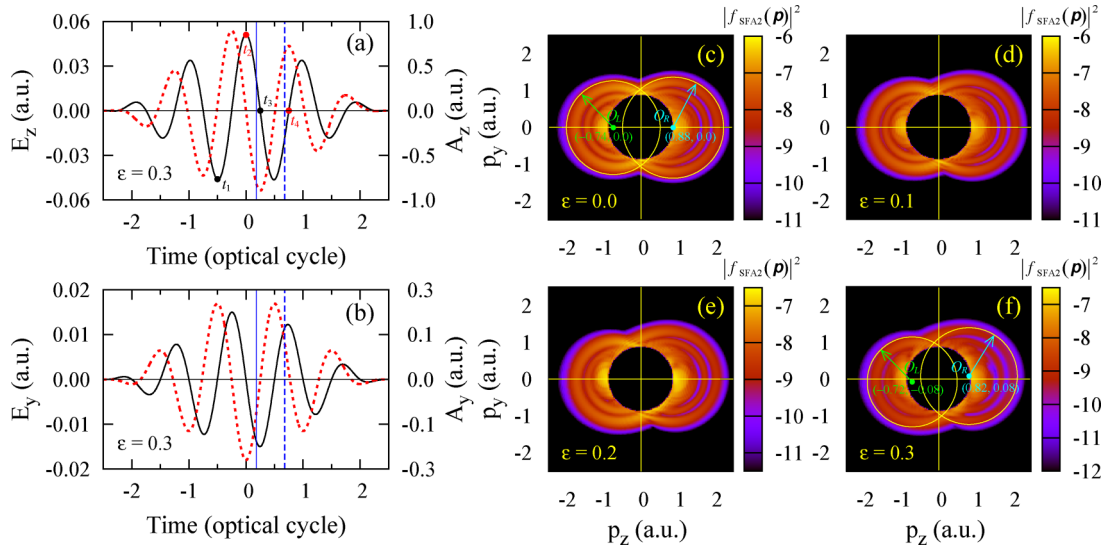
FIG. 3. (a,b) Same as Figs. 2(a) and 2(b), respectively, but for five optical cycles. (c)–(f) Two-dimensional photoelectron momentum distributions in the polarization plane with photoelectron energy larger than $2U_p$ for single ionization of atomic hydrogen in a five-cycle elliptically polarized laser field at an intensity of 1×10^{14} W/cm^2 and a wavelength of 800 nm with ellipticities of 0.0, 0.1, 0.2, and 0.3, respectively. The results are obtained from SFA2. In panel (f) the right- and left-side circles with the centers slightly above and below the major polarization axis represent the elastic scattering of a returning electron with the parent ion at recollision times before t_3 and t_4, respectively.

zero crossing as marked by the vertical lines in Figs. 2(a) and 2(b). This contradicts the conclusion drawn in [17,18] from the asymmetry pattern in experimentally measured correlated electron momentum distributions for NSDI of Ne in elliptically polarized fields. The simulations based on the semiclassical model show that multiple-return-collision dominates the contribution to NSDI by elliptically polarized fields while for linear polarization single-return-collision makes the dominant contribution [17]. Furthermore, by tracking the electron trajectories Kang *et al.* [17] found that, with increasing ellipticity, the recollisions occurring after the E_z zero crossing became more and more important in contributing to NSDI. Very recently, the observed asymmetry pattern in the correlated momentum distributions for NSDI of Ne in elliptically polarized fields was well reproduced by using the improved quantitative rescattering (QRS) model [19] based on the assumption that laser-induced recollisions take place after the E_z zero crossing for NSDI in elliptically polarized fields. However, it should be noted that the QRS model itself cannot be used to identify the recollision time without the hint from experiment.

As displayed in Fig. 2(c), less electrons tend to be accumulated in the outer ridges in the PMD in elliptically polarized field compared to the case of linear polarization [see Fig. 1(b)], which is consistent with the findings based on the three-dimensional semiclassical model [13]. By tracing the respective tunnel-ionized electron trajectory, Yu *et al.* [13] decoupled the contribution of the first and second recollisions in the PMDs and found that the relatively weaker distribution in the outer ridges in the PMD in the elliptically polarized field was attributed to the relatively decreased contribution of the first recollision to the outer ridge and the increased contribution of the second recollision to the inner ridge in the elliptically polarized field. However, our results in Figs. 1(b) and 2(c) are evaluated by using three-cycle laser

pulses, which indicates that the multiple recollision process is absent.

The transition from the linearly polarized to elliptically polarized laser fields in HATI of H is illustrated in Fig. 3. Here we use five-cycle laser pulses with ellipticities in the range from 0.0 to 0.3. Compared to three-cycle pulses, five-cycle pulses produce bigger left-side circular rings owing to the fact that the value of the vector potential at the recollision time around t_4 for five-cycle pulses is larger than that for three-cycle pulses, as shown in Figs. 3(a) and 3(b) and Figs. 2(a) and 2(b), respectively. It should be noted that the recollisions occurring about one cycle before the times around t_3 and t_4 play no role in forming the circular rings since the corresponding ionization rates at the times about one cycle earlier before the times around t_1 and t_2 are relatively too low. One can see from Figs. 3(c) to 3(f) that by increasing the ellipticity the centers of both the left- and right-side circles move slightly more and more off the major polarization axis due to the increase of the vector potential along the minor axis.

It should be noted that the ring structures in the PMD are not narrow such that the determination of the center of the ring is sensitive to both the size and the width of the ring. Actually, the recollision takes place within a time window corresponding to a time window of ionization, leading to a distribution in the momentum space. As a result, there exists a lot of back rescattering rings with different centers, as demonstrated in Fig. 5 in [24] for linear polarization. However, no matter the size of the back rescattering ring, the centers of the right- and left-side circles always move slightly off the major axis to the first and third quadrants, respectively.

We also performed the SFA2 calculations using longer laser pulses. In Fig. 4, we show the PMDs for HATI of hydrogen in both linearly and elliptically polarized laser fields with a full pulse duration of ten cycles. It can be found that the 2D photoelectron momentum spectra for HATI always
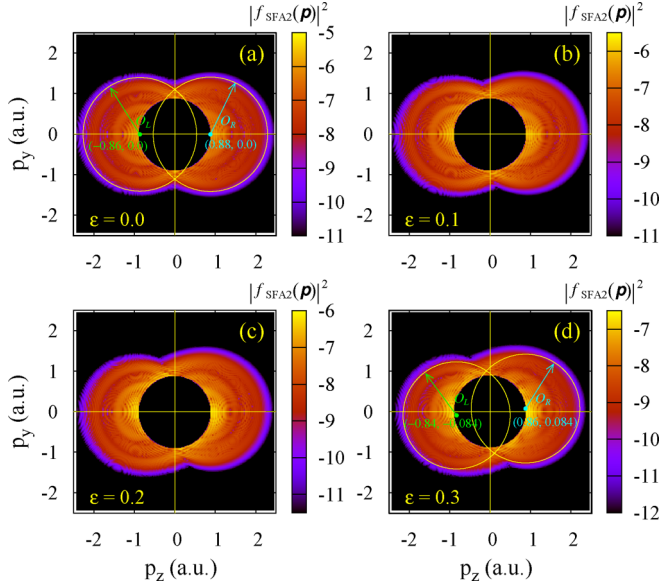
FIG. 4. Two-dimensional photoelectron momentum distributions in the polarization plane with photoelectron energy larger than $2U_p$ for single ionization of atomic hydrogen in a ten-cycle elliptically polarized laser field at an intensity of 1×10^{14} W/cm^2 and a wavelength of 800 nm with ellipticities of (a) 0.0, (b) 0.1, (c) 0.2, and (d) 0.3. The results are obtained from SFA2.

have the characteristic shape of a figure eight that is slightly distorted for elliptical polarization. In addition, with the elliptically polarized laser field given in Eq. (1), the center of the right-side (left-side) circle always moves up (down) to the first (third) quadrant. This indicates that the recollision
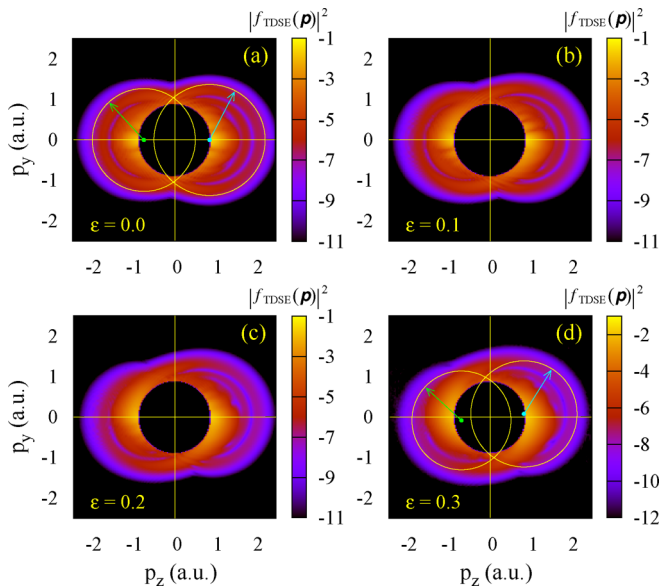

FIG. 5. Two-dimensional photoelectron momentum distributions in the polarization plane with photoelectron energy larger than $2U_p$ for single ionization of atomic hydrogen in a five-cycle elliptically polarized laser field at an intensity of 1×10^{14} W/cm^2 and a wavelength of 800 nm with ellipticities of (a) 0.0, (b) 0.1, (c) 0.2, and (d) 0.3. The results are obtained by solving the TDSE.

time can be unambiguously identified by analyzing the center shift of the measured PMDs for HATI in elliptically polarized fields.

Using the same laser parameters as in Fig. 3 we also obtained the PMDs for HATI of H by solving the TDSE and the results are displayed in Fig. 5. The arrows in Figs. 5(a) and 5(d) are the same as those in Figs. 3(c) and 3(f), respectively. Different from SFA2, the TDSE results consist of contributions of both direct ionization and rescattering. However, the high-energy part of the PMDs from TDSE still bear a striking resemblance to those from SFA2 due to the fact that direct ionization only dominates the low-energy spectra. Of course, for other atoms the discrepancies between SFA2 and TDSE do exist in the high-energy PMDs. This is because elastic scattering of the returning electron with the parent ion is treated in SFA2 approximately within the plane-wave Born approximation such that the information of the target structure is lost. Even so, the results of SFA2 for the PMDs of HATI can still serve as a powerful tool for probing the subcycle dynamics of the recollision process in elliptically polarized laser pulse since the shift of the center of the rescattering circle that is always a measure of the vector potential $\boldsymbol{A}_r$ at the recollision time does not depend on the atomic structure. In that sense, the SFA2 results of HATI in elliptically polarized laser pulse can be somehow regarded as experimental measurements from which the recollision time can be retrieved. Furthermore, although the TDSE provides the most accurate results, the calculations are extremely formidable for long laser pulses at high intensities and the results alone would not offer much insight into the basic mechanisms. Therefore, for the current purpose the SFA is preferred.

IV. CONCLUSION AND OUTLOOK

We present a theoretical study on subcycle dynamics of the recollision process in high-order above threshold ionization (HATI). The two-dimensional photoelectron momentum distributions (PMDs) for HATI of H by intense elliptically polarized laser pulses are calculated by using the strong-field approximation (SFA) and solving the time-dependent Schrödinger equation (TDSE). We demonstrate that the PMDs from both SFA and TDSE exhibit the characteristic shape of a figure eight that is slightly distorted for elliptical polarization. It is found that with increasing ellipticity, the centers of the rescattering circles move slightly more and more off the major polarization axis. Based on a simple analysis of the ellipticity-dependent center shift of the rescattering circles, it can be deduced that the favorite recollision times are *before* the zero crossing of the electric field along the major polarization. Our work indicates that, with the help of elliptically polarized laser pulses, the recollision time in HATI can be unambiguously identified.

The identification of the recollision time is based on the relation between the recollision time and the vector potential at that time. Here, we assume that the drift momentum is only determined by the vector potential at the recollision time, i.e., $\boldsymbol{p}_{\text{drift}} = -\boldsymbol{A}(t_r)$. Of course, in a real situation, this relation could be modified by the Coulomb effect with a small offset. Nevertheless, for the strong fields considered in this work, since the centers and the sizes of the rescattering

rings predicted by the SFA are in very good agreement with those obtained by solving the TDSE, it is reasonable to believe that the Coulomb effect on the drift momentum is negligible.

It should be noted that the correlated-electron and doubly charged ion momentum spectra from nonsequential double ionization (NSDI) of neon by intense elliptically polarized laser pulses were recently measured by Kang *et al.* [17] and the observed asymmetry of correlated electron and ion momentum distributions reveal that the recollisions in NSDI were more likely to occur *after* the zero crossing of the electric field along the major polarization for higher ellipticities, which

contradicts with what we found for HATI. To unveil the physical origin of this difference, further studies both theoretically and experimentally are highly desirable.

[1] P. H. Bucksbaum, M. Bashkansky, and D. W. Schumacher, Phys. Rev. A **37**, 3615 (1988).

[2] T. Brabec and F. Krausz, Rev. Mod. Phys. **72**, 545 (2000).

[3] F. Krausz and M. Ivanov, Rev. Mod. Phys. **81**, 163 (2009).

[4] J. L. Krause, K. J. Schafer, and K. C. Kulander, Phys. Rev. Lett. **68**, 3535 (1992).

[5] P. Colosimo, G. Doumy, C. I. Blaga, J. Wheeler, C. Hauri, F. Catoire, J. Tate, R. Chirla, A. M. March, G. G. Paulus, H. G. Muller, P. Agostini, and L. F. Dimauro, Nat. Phys. **4**, 386 (2008).

[6] Th. Weber, H. Giessen, M. Weckenbrock, G. Urbasch, A. Staudte, L. Spielberger, O. Jagutzki, V. Mergel, M. Vollmer, and R. Dörner, Nature (London) **405**, 658 (2000).

[7] B. Feuerstein, R. Moshammer, D. Fischer, A. Dorn, C. D. Schröter, J. Deipenwisch, J. R. Crespo Lopez-Urrutia, C. Höhr, P. Neumayer, J. Ullrich, H. Rottke, C. Trump, M. Wittmann, G. Korn, and W. Sandner, Phys. Rev. Lett. **87**, 043003 (2001).

[8] M. Busuladžić, A. Gazibegović-Busuladžić, and D. B. Milošević, Phys. Rev. A **80**, 013420 (2009).

[9] A. N. Pfeiffer, C. Cirelli, A. S. Landsman, M. Smolarski, D. Dimitrovski, L. B. Madsen, and U. Keller, Phys. Rev. Lett. **109**, 083002 (2012).

[10] M. Li, Y. Liu, H. Liu, Q. Ning, L. Fu, J. Liu, Y. Deng, C. Wu, L.-Y. Peng, and Q. Gong, Phys. Rev. Lett. **111**, 023006 (2013).

[11] X. Y. Lai and C. F. Faria, Phys. Rev. A **88**, 013406 (2013).

[12] X. Y. Lai, C. L. Wang, Y. J. Chen, Z. L. Hu, W. Quan, X. J. Liu, J. Chen, Y. Cheng, Z. Z. Xu, and W. Becker, Phys. Rev. Lett. **110**, 043002 (2013).

[13] J. Yu, X. Sun, Y. Shao, M. Li, Q. Gong, and Y. Liu, Phys. Rev. A **92**, 043411 (2015)

[14] Y. L. Wang, S. G. Yu, X. Y. Lai, X. J. Liu, and J. Chen, Phys. Rev. A **95**, 063406 (2017).

[15] H. Xie, M. Li, S. Luo, Y. Li, Y. Zhou, W. Cao, and P. Lu, Phys. Rev. A **96**, 063421 (2017).

[16] D. B. Milošević and W. Becker, Phys. Rev. A **105**, L031103 (2022).

[17] H. Kang, K. Henrichs, M. Kunitski, Y. Wang, X. Hao, K. Fehre, A. Czasch, S. Eckart, L. Ph. H. Schmidt, M. Schöffler, T. Jahnke, X. Liu, and R. Dörner, Phys. Rev. Lett. **120**, 223204 (2018).

[18] H. P. Kang, K. Henrichs, Y. L. Wang, X. L. Hao, S. Eckart, M. Kunitski, M. Schöffler, T. Jahnke, X. J. Liu, and R. Dörner, Phys. Rev. A **97**, 063403 (2018).

[19] F. Liu, S. Li, Z. Chen, B. Böning, and S. Fritzsche, Phys. Rev. A **106**, 043120 (2022).

[20] Z. Chen, S. Li, H. Kang, T. Morishita, and K. Bartschat, Opt. Express **30**, 44039 (2022).

[21] K. J. Schafer, B. Yang, L. F. DiMauro, and K. C. Kulander, Phys. Rev. Lett. **70**, 1599 (1993).

[22] P. B. Corkum, Phys. Rev. Lett. **71**, 1994 (1993).

[23] C. Jin, G. Wang, H. Wei, A.-T. Le, and C. D. Lin, Nat. Commun. **5**, 4003 (2014).

[24] Z. Chen, A.-T. Le, T. Morishita, and C. D. Lin, Phys. Rev. A **79**, 033409 (2009).

[25] M. Lewenstein, K. C. Kulander, K. J. Schafer, and P. H. Bucksbaum, Phys. Rev. A **51**, 1495 (1995).

[26] Z. Chen, T. Morishita, A. T. Le, and C. D. Lin, Phys. Rev. A **76**, 043402 (2007).

[27] T. Morishita, Z. Chen, S. Watanabe, and C. D. Lin, Phys. Rev. A **75**, 023407 (2007).

[28] V. N. T. Pham, O. I. Tolstikhin, and T. Morishita, Phys. Rev. A **99**, 013428 (2019).

[29] W. Becker, S. P. Goreslavski, D. B. Milošević, and G. G. Paulus, J. Phys. B: At. Mol. Opt. Phys. **51**, 162002 (2018).